DOI: 10.1002/anie.201205693

Since the Time of Robert Hooke

Advisory Board

Movies of Molecular Motions and Reactions: The Single-Molecule, Real-Time Transmission Electron Microscope Imaging Technique

*Eiichi Nakamura**

Keywords:
conformational analysis · molecular translation · real-time imaging · single-molecule imaging · transmission electron-microscope

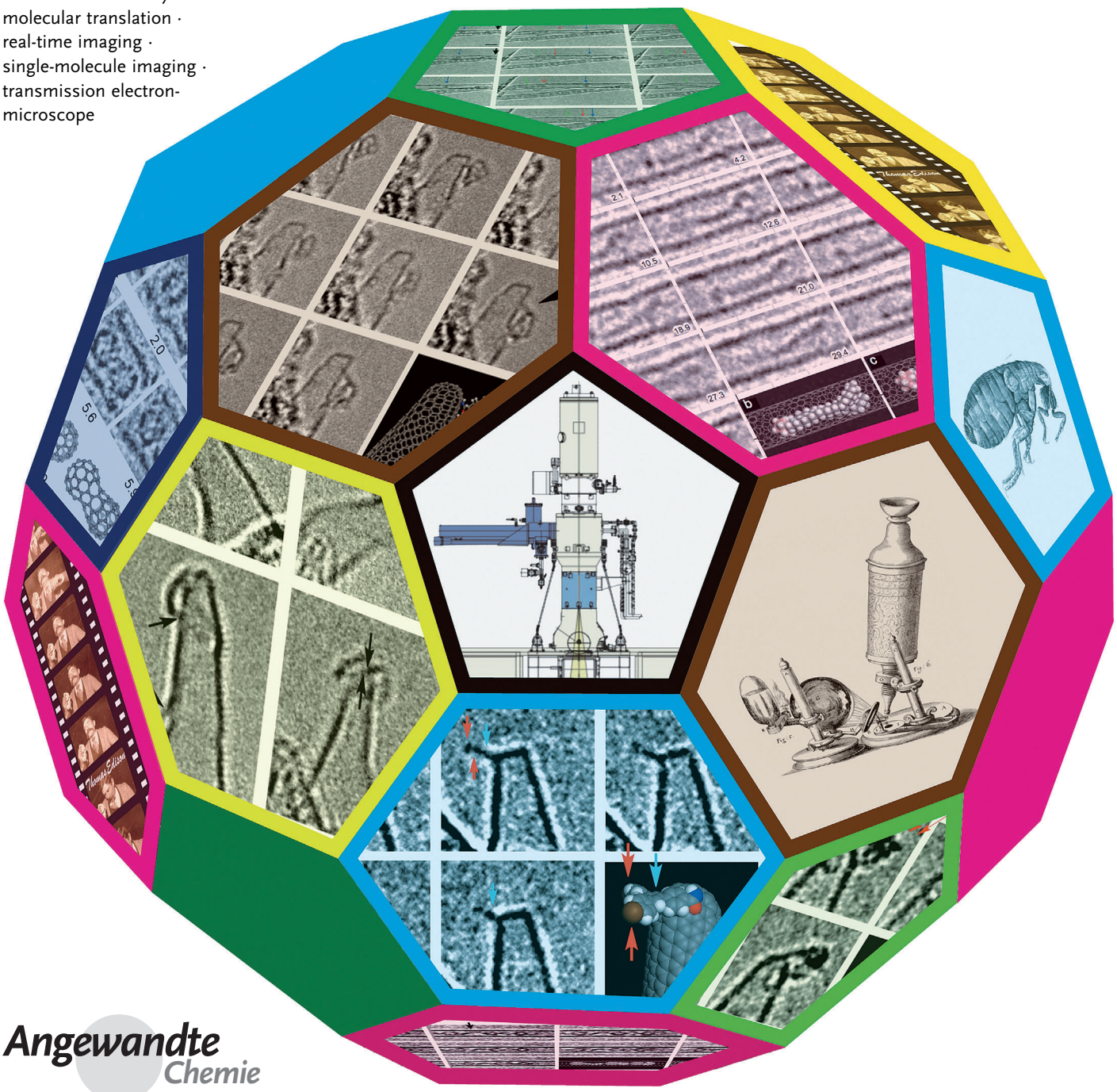

"The truth is, the Science of Nature has been already too long made only a work of the Brain and the Fancy: It is now high time that it should return to the plainness and soundness of Observations on material and obvious things," proudly declared Robert Hooke in his highly successful picture book of microscopic and telescopic images, "Micrographia" in 1665. Hooke's statement has remained true in chemistry, where a considerable work of the brain and the fancy is still necessary. Single-molecule, real-time transmission electron microscope (SMRT-TEM) imaging at an atomic resolution now allows us to learn about molecules simply by watching movies of them. Like any dream come true, the new analytical technique challenged the old common sense of the communities, and offers new research opportunities that are unavailable by conventional methods. With its capacity to visualize the motions and the reactions of individual molecules and molecular clusters, the SMRT-TEM technique will become an indispensable tool in molecular science and the engineering of natural and synthetic substances, as well as in science education.

From the Contents

1. Introduction

What was happening in the year 1888 when *Angewandte Chemie* was first published, 125 years ago? It was the time when Sachse was challenging Baeyer's proposal of flat cyclohexane,[1] and Edison was pondering on the invention of a motion picture exhibition device, the Kinetoscope. Seeing is believing. Wouldn't Sachse have dreamed of filming a molecular movie to prove that Baeyer was wrong?

After 125 years, molecular movies have emerged as a new tool in chemistry, and have visually illustrated the conformational mobility of organic molecules.[2,3] The motions and the reactions of a single organic molecule can be recorded on a CCD as they occur in the vacuum column of an atomic resolution transmission electron microscope (TEM). Thus, the single-molecule, real-time (SMRT) TEM imaging technique is opening up new horizons in chemistry. The technique consists of first, loosely binding a small molecule to a carbon nanotube, either by a chemical bond or by a weak van der Waals interaction, and then observing its motions and reactions with an atomic resolution TEM. This technique is finding use in the analysis of individual molecules and molecular clusters that are otherwise difficult to study by any conventional methods.

Since the initial discovery, first reported in the February 22, 2007 issue of *Science*,[4] we have published movies of a number of molecules, like those in Scheme 1. Just like an ordinary movie in the theater, the molecular movie is not best suited to analyzing the details of the recorded events. Therefore, in this Review, each frame of the movies will be printed so that we can fully enjoy viewing the molecular events recorded at atomic precision.

In the summer of 2004, I considered the feasibility of watching small organic molecules with TEM, and started the "Nakamura Functional Carbon Cluster ERATO Project", with financial support from the Japan Agency for Science and Technology. The consensus of the TEM community then was, however, that organic and biomolecules are too sensitive to be studied with a high resolution TEM.[5,6] In addition, there appeared to be rather scant interest in studying time-dependent phenomena with TEM. The project would not therefore have been possible without the collaboration of a world-class electron microscopist, Dr. Kazu Suenaga, as a group leader of the project, and with the help of the synthesis team headed by Dr. Hiroyuki Isobe.

2. The First Movie of Conformational Change of Alkyl Chains in Motion

To study the bond rotations and chemical reactions of organic molecules, the most naïve approach would be to collect information on three-dimensional structural change over time for many individual molecules. Information of such multi-dimensional quality cannot be obtained by spectroscopic or crystallographic methods. Microscopic methods can in principle provide such data, but in practice many of them

[*] Prof. E. Nakamura
Department of Chemistry, The University of Tokyo
Tokyo 113-0033 (Japan)
E-mail: nakamura@chem.s.u-tokyo.ac.jp

Supporting information for this article is available on the WWW under http://dx.doi.org/10.1002/anie.201205693.

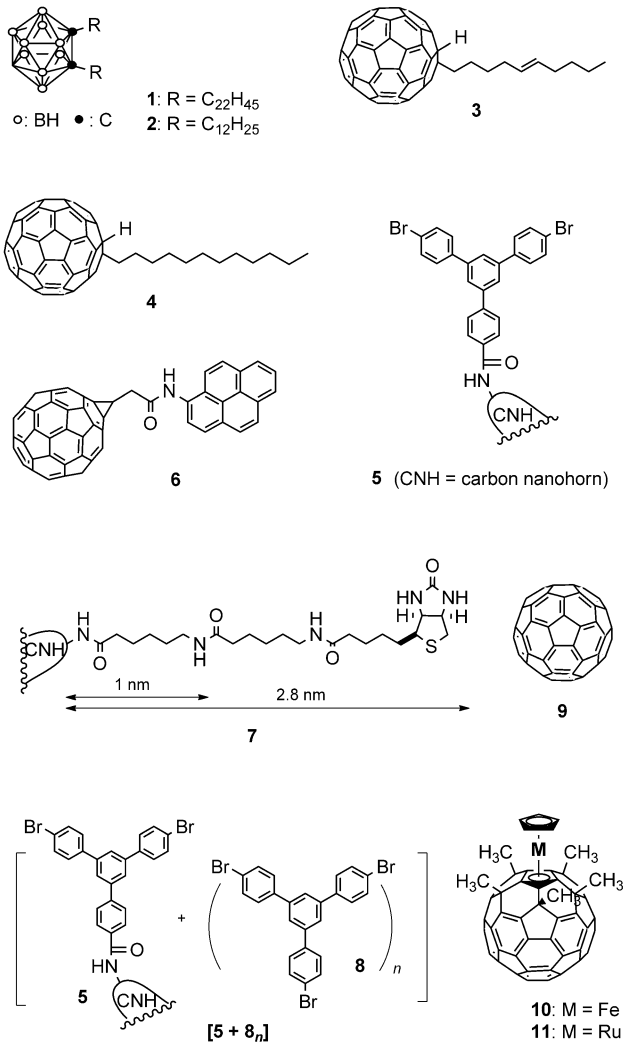

Scheme 1. Structures of molecules and molecular clusters studied by SMRT-TEM imaging.

do not. Scanning probe microscopy shows us sub-nm resolution 2D pictures of the molecules but lacks time resolution. High-resolution optical microscopy inherently lacks spatial resolution necessary for the study of bond rotations and chemical reactions. The capacity of TEM in this area has thus far been neglected because of the over-emphasized instability of organic molecules under irradiation. As we will see in this Review, the SMRT-TEM imaging technique provides the structural information of multi-dimensional quality for organic molecules of interest for chemists, biologists, and materials scientists. It has been particularly useful for the molecular-level studies of the events taking place at solid/liquid and solid/gas interfaces—a subject that is generally difficult to study experimentally.

Eiichi Nakamura received his Ph.D. in Chemistry at Tokyo Tech and became Professor of Chemistry at the University of Tokyo in 1995. He is the Program Director (Chair) at Japan Agency for Science and Technology (JST), and Visiting Professor of the Institute of Chemistry, Chinese Academy of Sciences in Beijing. His honors include The Chemical Society of Japan Award (2003), Humboldt Research Award (2006), The Medal with Purple Ribbon from His Majesty the Emperor of Japan (2009), and the Einstein Professorship of the Chinese Academy of Sciences. His research includes synthesis and physical organic chemistry, nanoscience, organic solar cells.

2.1. Conformational Change of Dialkyl Carboranes in a Carbon Nanotube

The first atomic resolution movie of an organic molecule in motion was recorded for the didocosanyl carborane **1** in a single-walled carbon nanotube (CNT) placed on the sample stage of a TEM operating at 293 K. Fourteen frames out of the movie of the conformational change of **1** over 35.7 s are shown in Figure 1.[2] Note that these images are the original CCD images and not computationally manipulated except for the normalization of the positions of the CNT that vibrated incessantly up and down by several Å on the time scale of seconds.

The molecules of **1** and CNTs (oxidized to remove the end caps prior to the experiment) were heated together in vacuum, then rinsed with solvent to remove the excess molecules from the exterior of the CNTs. A black powder of the molecule/CNTs was placed under a vacuum of 4×10^{-6} Pa on the sample stage of a JEOL JEM-2100F TEM with 2.3 Å spatial resolution at 120 kV acceleration voltage (Figure 2). A temperature of 793 K and an acceleration voltage of 80 kV were used when necessary. The minimum-dose system enabled us to acquire an image with an electron irradiation as low as 4.0×10^4 electron nm^{-2} (0.6 C cm^{-2}). For the movies taken at 4 K, we used a JEM-2100FC instrument equipped with an aberration corrector for the objective lens and a helium-temperature stage.

In addition to the unique shape of the molecules, the presence of the carborane group helped us to identify the molecules by electron energy loss spectroscopy (EELS)—a unique capability of TEM to identify the elemental composition of samples at a spatial resolution on the nm level.[7] Note that the EELS experiments may destroy the molecules because the information is obtained from inelastic collisions of the electron beam with the samples, whereas the SMRT-TEM images themselves originate from elastic collisions that have a very small cross section (with light atoms) and are essentially non-destructive. The lattice contrast of the background CNT may be eliminated mathematically to enhance the contrast of the internal molecules, or be eliminated entirely by placing the molecule in a vacuum outside the CNT (see Sections 4.2, 5.2, and 6). Note that the white bands surrounding the two side walls of the CNT as well as the molecule are Fresnel fringes that were caused by the phase change of the electron beam induced by interaction with the carbon atoms. This phenomenon conveniently enhances the contrast of the molecules, as we will see throughout this Review.

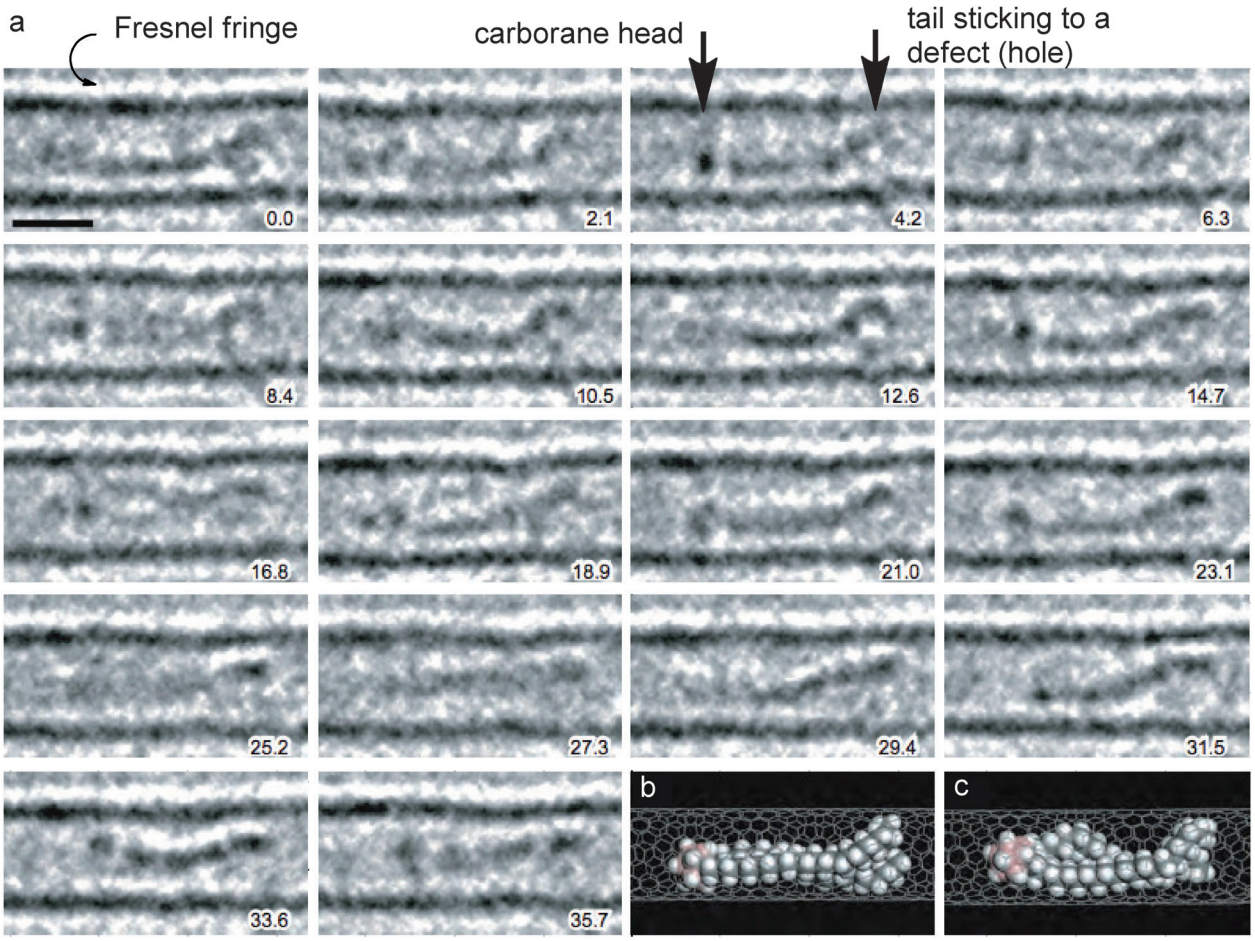

Figure 1. Time course of the conformational change of a single molecule of a carborane having two docosanyl ($C_{22}H_{45}$) tails (**1**) in a CNT of a 1.2 nm diameter on a 293 K sample stage in vacuum. The scale bar is 1 nm. The numbers at the bottom of each image show the time of the observation in seconds since the beginning of the electron irradiation of the specimen molecule. In this and other Figures, the frames are shown along the time course from left to right and from top to bottom. a) The images were obtained in an interval of 2.1 s with an electron irradiation time of 0.5 s followed by 1.6 s data readout time where there was no electron irradiation. This is the standard TEM condition throughout the present study. An acceleration voltage (E) was 120 kV and the total electron dose from the beginning of electron irradiation (0 s) until time 35.7 s was 6.8×10^5 electron nm^{-2}. b) and c) Molecular models of the image at times 4.2 s and 6.3 s, respectively. H white, B pink, C gray. The motion picture is shown in Movie S1 in the Supporting Information, and enlarged images are in Figure S1. Adapted from Ref. [4].

The movie of a single molecule of **1** is rich in structural information. First, the pictures tell us that the molecule has one head and two tails of a similar length that are visible in frames 6.3 and 16.8 s. Second, the molecule is approximately 3 nm in length (exact length depends on the angle between the specimen molecule and the electron beam). If we were previously informed that the molecule was an alkyl carborane, we can guess that it was a didocosanyl carborane. Third, only a limited number of conformational possibilities appear to be available to the molecule, and the conformational change is ratchet-like and stochastic, which nearly agrees with what we expect for C–C bond rotation. When the molecule moved rapidly during the 0.5 s irradiation time, the image was blurred as we find in many of the frames, and when we see well-defined images, as in frame 4.2 s, the molecule stayed in one position during the 0.5 s. Notably, however, the motions that we see in Figure 1 and all other movies occurred largely during the 1.6 s data retrieval time where there was no electron irradiation.

Our TEM system behaves like a poor digital camera with a very slow shutter speed of 0.5 s and a digital data retrieval time of 1.6 s. Therefore, the successful imaging of molecular motion was almost a miracle, given the common sense that the motions of a hydrocarbon occur on a picosecond time scale in vacuum. On the contrary, the conformational changes that we saw took place very slowly, on the time scale of seconds. On the basis of the results to be described in Section 3, we know that one of the two docosanyl tails was trapped in a structural defect (e.g., a hole) in the CNT wall. Therefore, we see the image of one tail very clearly on the right-hand side of each frame throughout the movie.

2.2. Three Alkenyl Chains Rotating in Parallel

Unlike the alkyl carborane in **1** that can interact only weakly with the π-surface of the CNT and hence tends to translate rapidly in the tube (Section 7.1), the fullerene

Figure 2. JEM-2100F, a TEM instrument used for the movie in Figure 1, is available in many institutions worldwide. A JEM-2100FC instrument equipped with an aberration corrector for the objective lens and a helium-temperature stage was used when necessary.

moiety in alkyl and alkenyl fullerenes **3** and **4** anchored the molecule in position and allowed us to further examine the conformational change and translation of these hydrocarbon groups.[8] Visualization of fullerene and endohedral metallofullerene derivatives had by this time been frequently reported because the discovery of "peapod" encapsulation (fullerene "peas" in a CNT "pod") was widely known from studies of fullerenes in CNTs.[9–12] Therefore, when mixed with an oxidized CNT in toluene, dec-5-enyl fullerene **3** spontaneously entered and stayed virtually motionless in a CNT, while the hydrocarbon tails moved during observation.

In Figure 3, we see three dec-5-enyl fullerene **3** molecules in three different conformations, or three different conformers of **3** (cf. molecular models). We can watch the three conformers changing their structure simultaneously and independently. We notice first that the decenyl chain in the left molecule (shown with an arrow) takes one conformation in the beginning and another in the second frame. The image of the alkenyl chain shown with a blue arrow looks like a superposition of the two conformers, suggesting that the molecule took two conformations during the 0.5 s exposure time. It appears that this molecule takes only two conformations, for some unknown reasons. The side chain of two other molecules shown with red arrows were folded tightly in the narrow tube, and moved much less during the observation.

3. Translation of an Alkyl Chain through a Hole in a CNT Wall

3.1. Partial Egression of an Alkyl Chain through a Hole

Gas storage in CNTs and molecular permeation through a graphene sheet have attracted considerable interest.[13] The SMRT-TEM technique has captured the motions of hydrocarbon molecules entering and leaving a CNT, giving us a molecular image of the way molecules may pass through a small hole pierced in a thin substance—an image that would not have been possible to create by other experimental methods.

Figure 4 illustrates a TEM view of partial egression of the dec-5-enyl chain of **3** into the vacuum through a hole defect.[8] The rotating alkenyl chain partially left the hole, and stayed in one conformation (white boxes) in the middle for about 15 s before it came back again into the tube. Was there any specific interaction between the olefinic bond and the hole? It is a question of rather unusual caliber, but may be answered by a theoretical method.

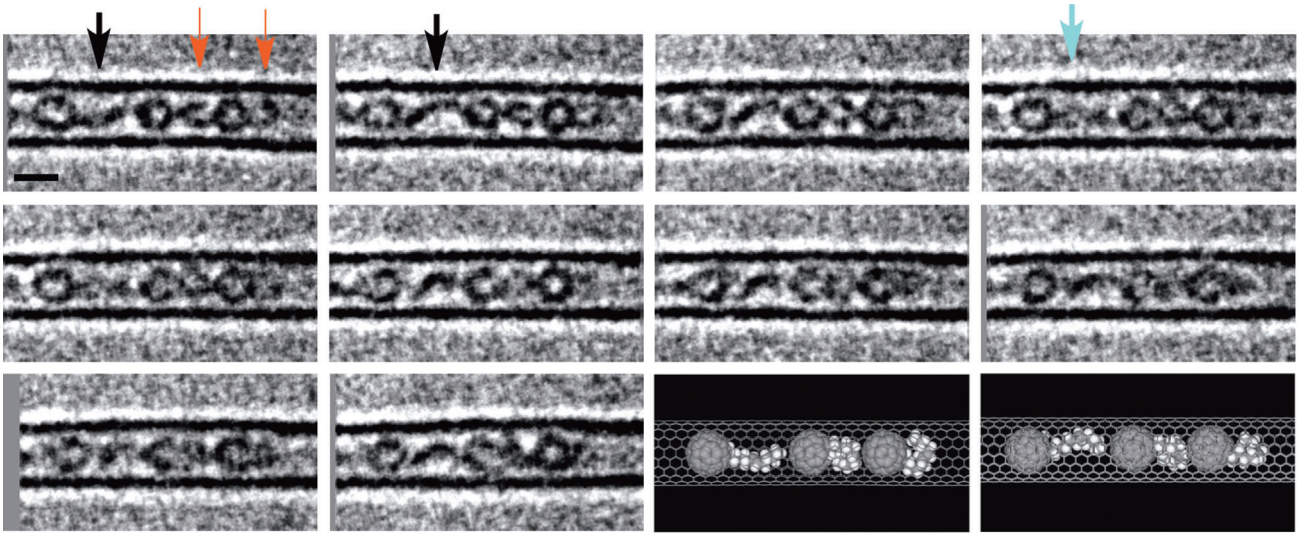

Figure 3. Dec-5-enyl [60]fullerene **3** in a CNT at 293 K as observed for 0.5 s with a time interval of 6.3 s ($E = 120$ kV). TEM images for a total of 63 s, and molecular models of different conformers. The total electron dose during the observation was 1.1×10^6 electron nm^{-2}. Scale bar is 1 nm. The motion picture is shown in Movie S2, and enlarge images are in Figure S2. Adapted from Ref. [8].

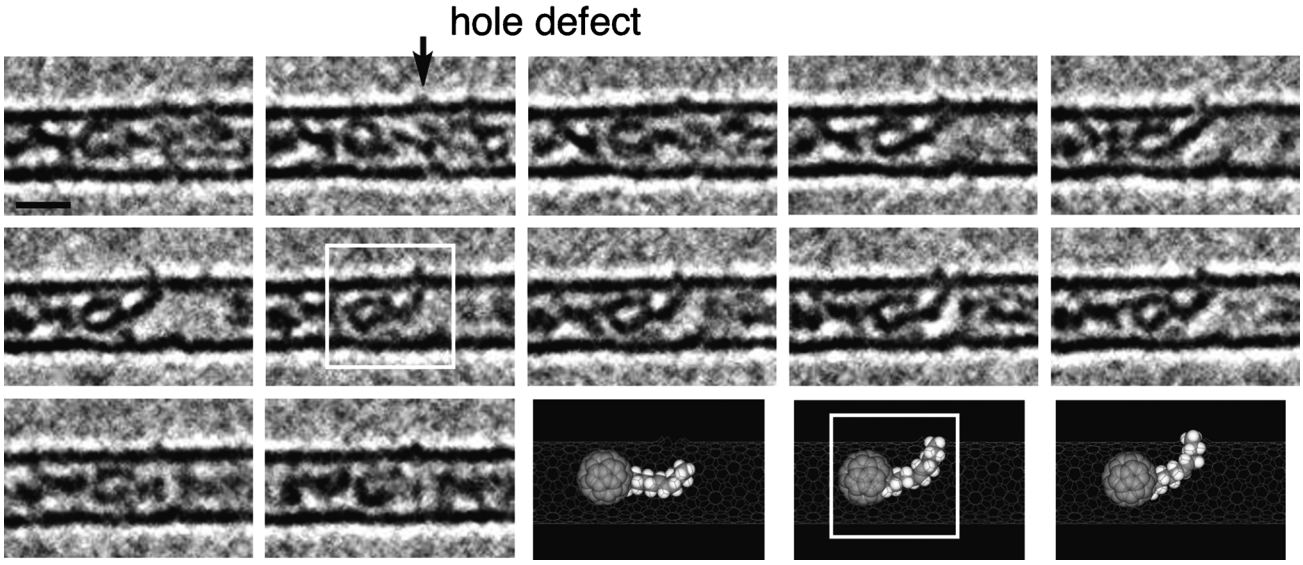

Figure 4. Dec-5-enyl [60]fullerene **3** in a carbon nanotube, as observed with a time interval of 2.1 s ($E = 120$ kV). Sequential TEM images of alkenyl fullerene captured over a period of 25.4 s on a sample stage at 293 K, and the corresponding molecular models. The total electron dose during the observation was 4.8×10^5 electron nm^{-2}. The motion picture is shown in Movie S3, and enlarged images are in Figure S3. Adapted from Ref. [8].

3.2. Egression into Vacuum at 4 K

In Figure 5, we show three molecules of dodecyl [60]fullerene **4** at 4 K (cf. the molecular models).[8] As indicated by an arrow, there was a defect in the tube wall, and that is where the alkyl chain was squeezed out of and pushed back into during about 10 s, as we see in the second row of pictures. There are two notable issues. First, this translation of the alkyl chain took place along the molecular axis and the chain remained linear throughout the egression and reentry. Second, the speed of the molecular motions observed here on the 4 K stage is qualitatively similar to that observed for the samples at 293 K discussed in Section 3.1.

As we will see throughout this Review, the molecular motions were found to be extremely insensitive to the temperature of the sample stage: The motions neither stopped at 4 K, nor became too violent at 793 K. Thus, the motions of single molecules loosely connected to a CNT in vacuum did not follow the Arrhenius equation. This empirical equation was developed to describe the behavior of molecular ensembles under thermally equilibrated conditions and clearly cannot be applied to a single molecule placed on or in a CNT in high vacuum.

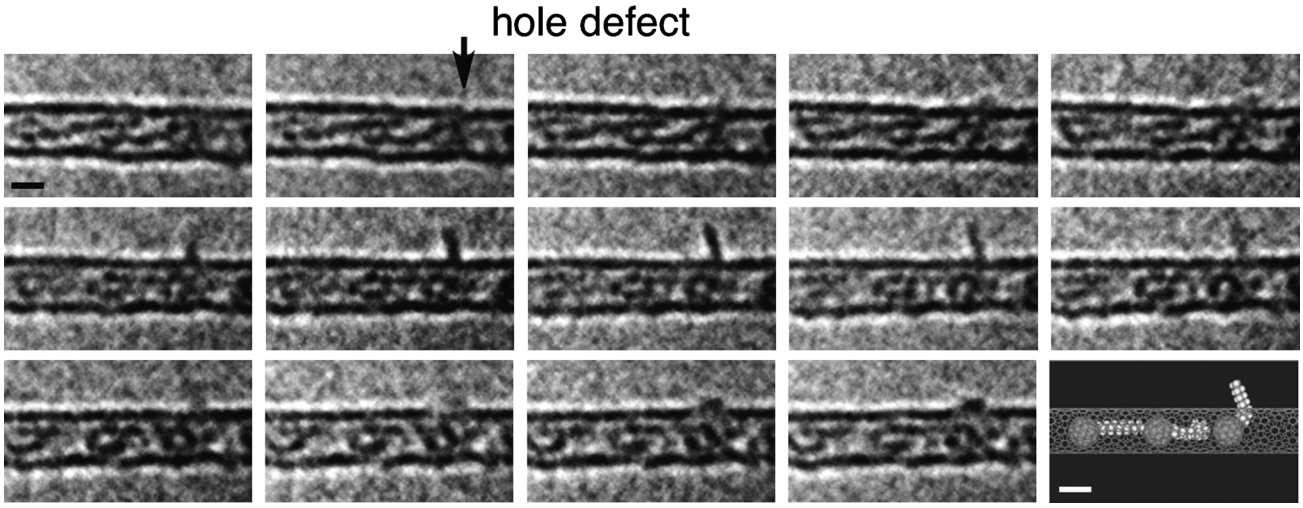

Figure 5. Dodecyl [60]fullerene **4** in a CNT on a sample stage at 4 K as observed with a time interval of 4.2 s ($E = 120$ kV; resolution of 2.6 Å). Sequential TEM images of alkyl fullerene captured over a period of 58.8 s, and the corresponding molecular model. Scale bars are 1 nm. The nanotubes have a diameter of 1.4 nm. The TEM images were obtained with a JEOL JEM-2100FC TEM with an aberration corrector and a helium temperature stage, and the total electron dose during the observation was 4.1×10^6 electron nm^{-2}. The motion picture is shown in Movie S4, and enlarged images in Figure S4. Adapted from Ref. [8].

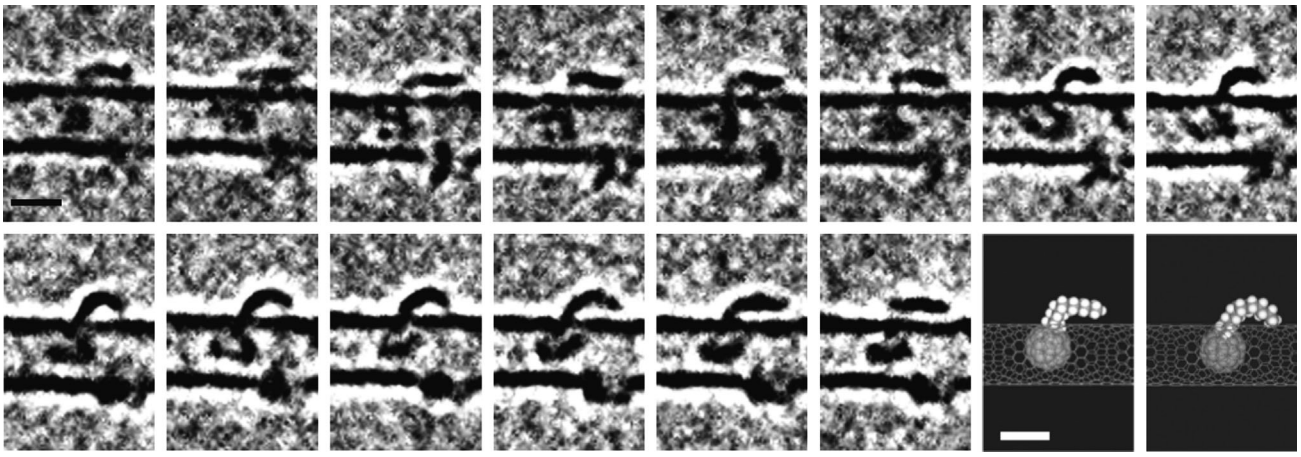

Figure 6. Slow motion of a dodecyl group of the fullerene molecule **4** on a 293 K sample stage as observed with a time interval of 2.1 s ($E = 120$ kV). TEM images and molecular models. The total electron dose during the observation was 5.6×10^5 electron nm^{-2}. The motion picture is shown in Movie S5, and enlarged images in Figure S5. Adapted from Ref. [8].

4. Very Slow C–C Bond Rotation in Vacuum

4.1. van der Waals Interactions in Vacuum

The dodecyl chain of **4** on the 4 K sample stage in Figure 5 did not change its linear conformation for 9 s. How fast does the alkyl chain in vacuum move on a 293 K stage? Figure 6 illustrates the alkyl chain of **4** entirely in vacuum that touches the exterior wall of the CNT.[8] The dodecyl chain moved very slowly and retained van der Waals contact with the CNT surface throughout the observation period of about 1 min. Because the energy gain by the van der Waals interaction is in the order of several kcal mol^{-1}, we can conclude that the molecule received a very small energy for vibration of the alkyl chain either from the electron beam or from the environment of the TEM.

4.2. Slow Rotation of Biphenylamide in Vacuum

To study the speed of the bond rotations free from interference by the CNT, we constructed a system where a molecule stands upright in the vacuum space on the CNT surface.[14] Being aware of the rigidity of a benzamide linkage, we synthesized a dibromobenzamide on a carbon nanohorn (**5**; CNH),[15] a tapered variant of a single-wall CNT (Figure 7). The characteristic Y shape of the dibromobenzamide molecule, as well as the presence of the bromine atoms, facilitated the structural determination of the conformers. In addition, by placing the molecules on the surface of a nanotube, we can obtain a better image contrast than placing them in its interior.

As shown by the images in Figure 7 taken on the stage at 293 K, the bottom half of the molecule (up to the light-blue arrow) is inflexible and hence visible throughout the observation. The two rotating bromophenyl groups (red arrows) on the other hand are blurred and invisible most of the time except in two frames where they can be identified. This and other movies taken either at 4 K or at 293 K indicated that the C–C bond rotation is largely insensitive to temperature, and does not stop, even at 4 K. The molecule stayed in one or a few stable conformations at least 4 to 10 times per minute. Development of TEM imaging methods with higher time resolution[16] will lead to dramatic improvement in the image resolution of such quickly rotating molecules, and broaden the applicability of the SMRT-TEM technique.

5. Conformational Change of Molecules of Some Complexity

It was amazing that we saw the motions of hydrocarbons. How about imaging more complex functional groups, such as an amide, a ubiquitous and important group in proteins? As shown in Figure 8, we were able not only to see a C=O group in an amide group, but to study the conformational behavior for the first time.[17] We can see very clearly the image of an aromatic ring as small as a pyrene ring. A recent report showed the static side view of the coronene ring, illustrating the utility of SMRT-TEM for structure determination of aromatic compounds.[18]

5.1. Planar Conformation of the 6-Pyreneamide Linkage

Figure 8 illustrates a molecule of some complexity, an *N*-pyrenyl fullerene amide **6**.[17] This molecule features a fullerene moiety that anchors the molecules stably in a CNT, a conformationally rigid pyrene amide moiety, and a mobile methylene group connecting these groups. The fullerene core sometimes appears ellipsoidal, probably because of vibration along the tube axis during the exposure time. Comparison with a TEM simulation based on the molecular models in the bottom right panels of Figure 8 allows us to assign the dark dot next to the fullerene circle as the C=O group that lies parallel to the electron beam. The molecular image is most

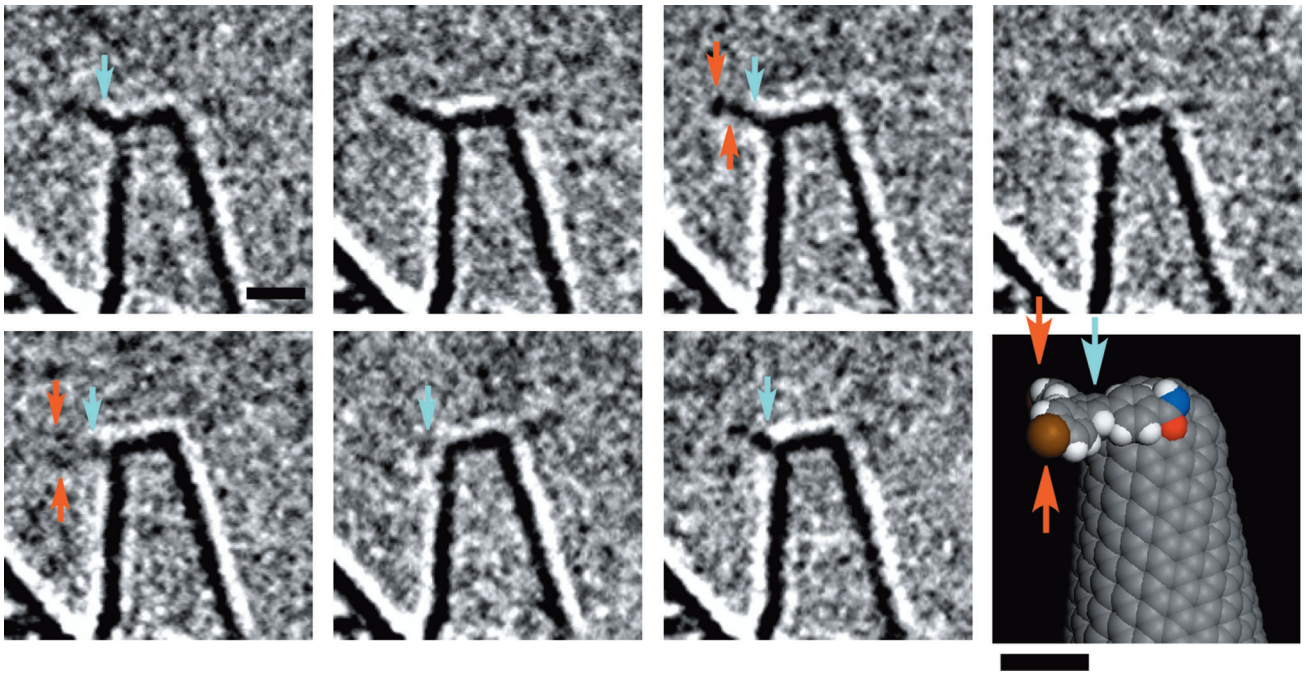

Figure 7. Dibromophenylbenzamide on a carbon nanohorn (**5**) as observed with a time interval of 2.1 s ($E = 120$ kV). The total electron dose during the observation was 2.5×10^5 electron nm^{-2}. Red arrows and light-blue arrows indicate the bromophenyl and the central benzene groups, respectively. Scale bars are 1 nm. Br orange, O red, N blue. The motion picture is shown in Movie S6, and enlarge images in Figure S6. Adapted from Ref. [14].

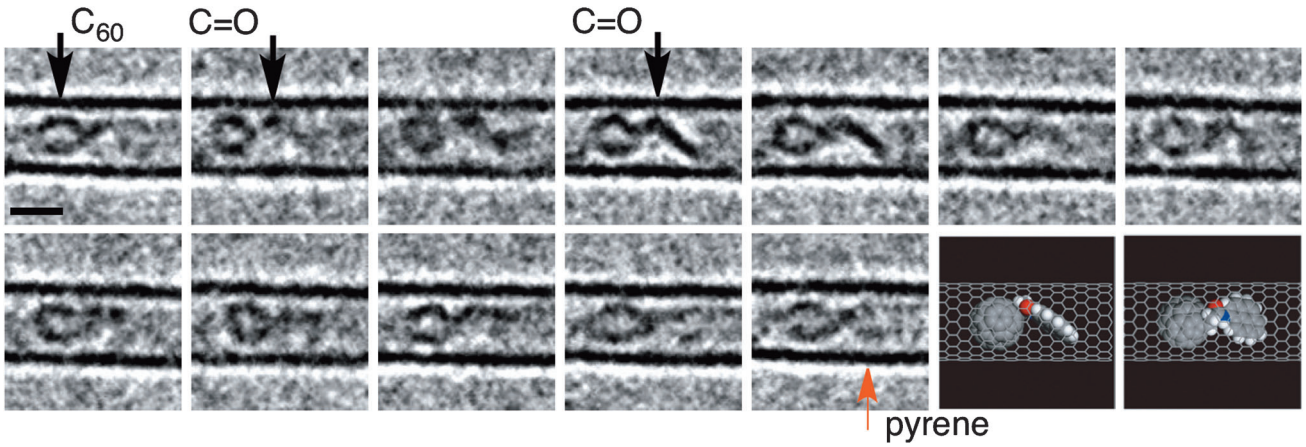

Figure 8. *N*-Pyrenyl fullerene amide **6** in a 1.4 nm diameter CNT as observed with a time interval of 4.2 s ($E = 120$ kV). The total electron dose during the observation was 9.2×10^5 electron nm^{-2}. Scale bar is 1 nm. The motion picture is shown in Movie S7, and enlarged images in Figure S7. Adapted from Ref. [17].

clearly seen in the middle of the first row when the pyrene ring is seen from the side and the C=O group along the C–O axis. These images are clear enough to allow us to visually determine the structure, where the amide group shares the plane of symmetry with the pyrene ring. This is the most stable conformer available for such a pyrene amide. In the middle of the observation, the molecule started to change its conformation, probably because of rotation of the methylene group, and exposed the top side of the pyrene group to the viewer (red arrow).

5.2. Sampling of Local Conformational Minima

We next probed the capability of SMRT-TEM imaging in the analysis of a more complex substrate, a biotinyl triamide **7**.[19] As with the Y-shaped molecule on a CNH **5**, we connected the molecule to a CNH by an amide bond. As illustrated by the six images in Figure 9, we could detect a few triamide molecules on each CNH that are attached mostly to the curved regions of the CNH. These images thus provided the first direct experimental support for the accepted view that the most strained regions of a CNT and CNH are more

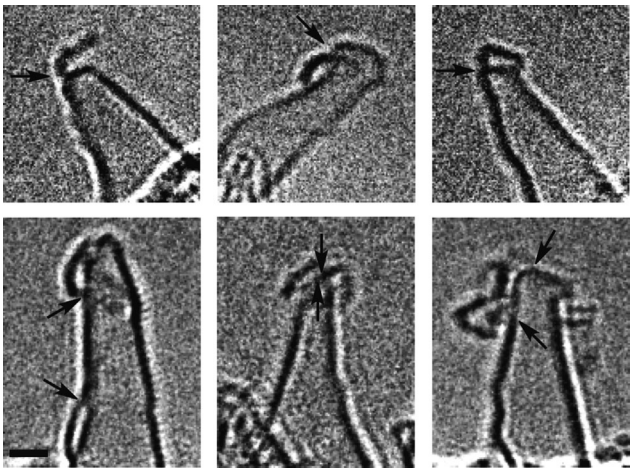

Figure 9. A mixture of various conformers of biotinyl triamide **7** on CNHs ($E = 120$ kV). Arrows indicate the positions of the basal amide bonded to the CNH surface. Identification of such positions could be made more easily on movie images than on still images. Scale bar is 1 nm. Reprinted with permission from Ref. [19]. Copyright 2008 American Chemical Society.

reactive than the sidewalls.[20] Each conformer is located in a kinetically separated local minimum, and most of them underwent very small conformational changes in each potential well. This observation is additional evidence that the molecules receive very little vibrational energy under the SMRT-TEM conditions. The basal amide group indicated by a black arrow connects the biotin and the CNH, and hence did not change its position, while the remaining part of the molecule moved slowly (Sections 5.3 and 5.4).

5.3. Stretching Motion of the Biotin Triamide Chain

The motion of the biotin triamide **7** is exemplified with six frames of the movie showing a bent conformer and recorded for about two minutes (Figure 10a).[19] From the picture we can extract three pieces of information. First, the molecule is bonded to the cap of the CNH and stretches to the right, keeping contact with the CNH surface (see the molecular model, Figure 10b). Second, the structural change occurs smoothly and in a stepwise manner from one conformer to another, as illustrated by the images that are mutually related, and occur one after another. Finally, the conformational change is slower than what we saw for the hydrocarbon in a CNT in Figure 1. This slower change is in good agreement with the rigidity of the amide bonds. It is, however, difficult to draw any quantitative conclusion on the speed of molecular motion based on the movie image of single molecules.

The dark spots indicated by arrows in Figure 10a are due to overlapping carbon, nitrogen or oxygen atoms, and serve as markers that assist structure assignment. As seen by the positions of the biotin terminus indicated by black arrows, this conformer did not change its structure very much and stayed in one local conformational minimum throughout the observation. The agreement of the TEM image (Figure 10a) and the simulated image (Figure 10c) based the molecular model

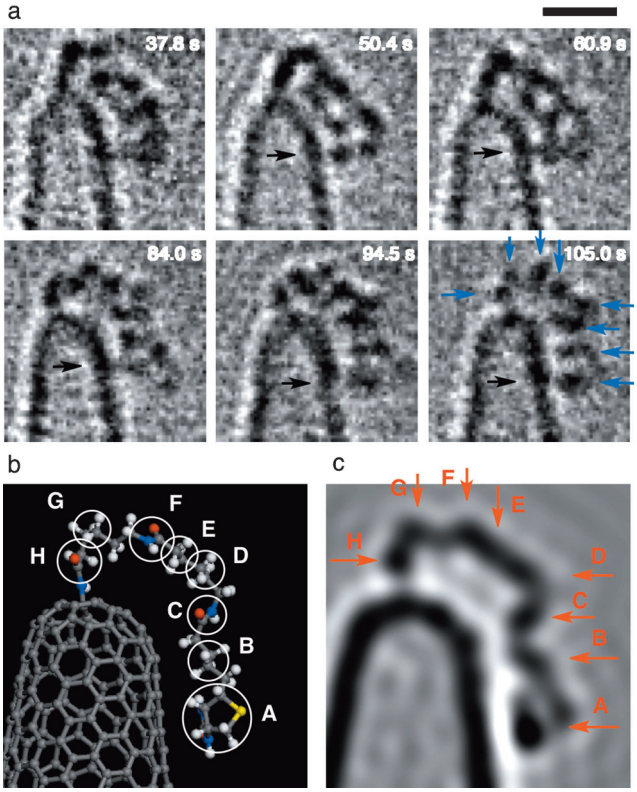

Figure 10. Biotin triamide **7** changing its structure through a sequence of bent conformations. a) SMRT-TEM images ($E = 120$ kV). The captions refer to the time (seconds) after the start of the observation, that is, the start of electron irradiation. b) and c) Molecular structure of **7** and its simulated image at 105.0 s. The total electron dose from the beginning of electron irradiation (0 s) until time 105.0 s was 1.6×10^6 electron nm^{-2}. Scale bar is 1 nm. The motion picture is shown in Movie S8, and enlarge images in Figure S8. Reprinted with permission from Ref. [19]. Copyright 2008 American Chemical Society.

(Figure 10b) as to the dark spots A–H indicates that the model structure shown is a likely conformer that gave the experimental TEM image. In this way, we can obtain a reasonable guess as to the conformation of **7**, for which there are over 10^8 possibilities available.

5.4. Hydrogen-Bond Reorganization of Biotin Triamide

Figure 11 shows another conformer of **7**, which underwent a much larger conformational change during observation over a few min.[19] This is a rare example in which we saw a conformational change from one minimum to another. The first picture illustrates a large cyclic form. As illustrated with a molecular model in the bottom right of Figure 11, this large cycle was probably formed by weak interactions between the biotin terminal and the basal amide group. The structure did not change much for some time (ca. 70 s), and then a large motion took place. The three pictures in the middle of Figure 11 are blurred and differ very much from each other, indicating the occurrence of continuous conformational changes occurring over about 6 s. This motion must have involved a significant change in hydrogen bonding and van

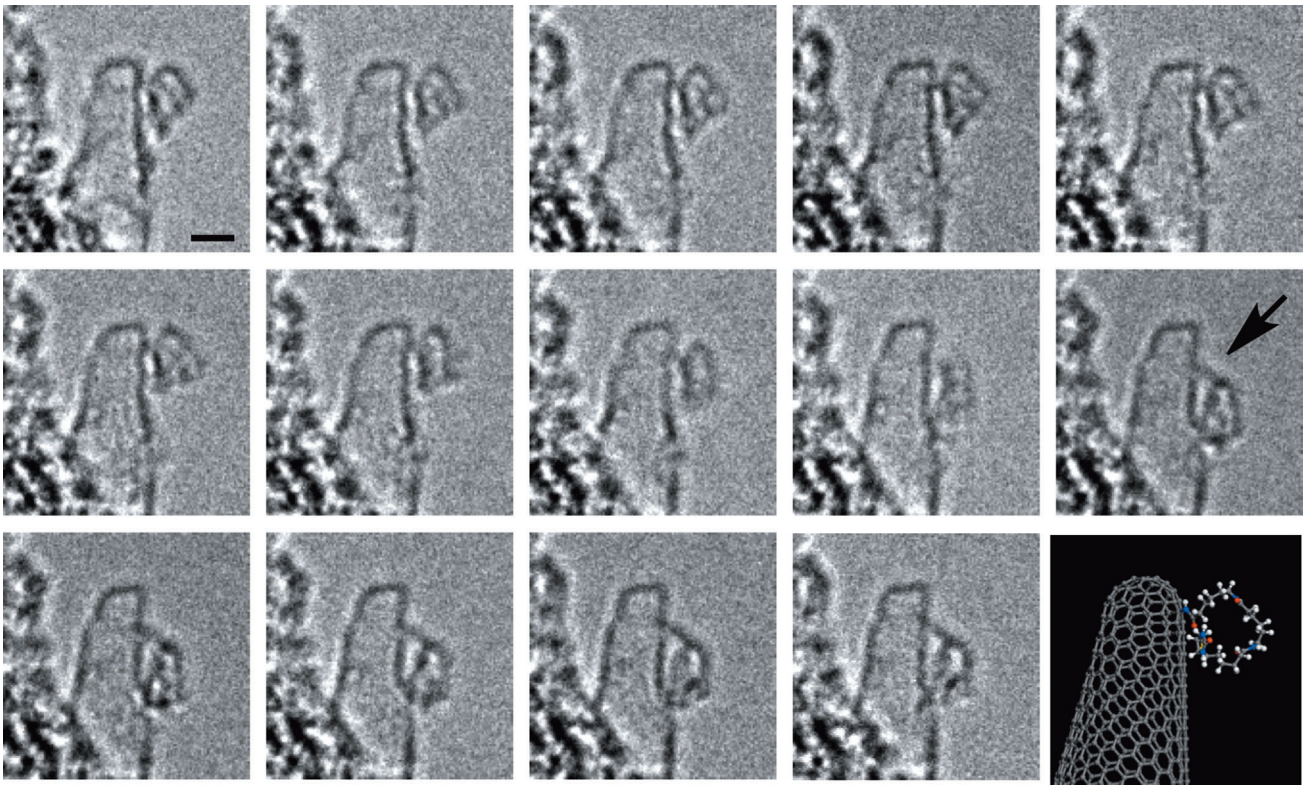

Figure 11. Biotin triamide **7** in cyclic conformations, as observed with a time interval of 2.1 s ($E = 120$ kV). The total electron dose during the observation was 2.9×10^5 electron nm^{-2}. The arrow indicates the $CO(CH_2)_5NH$ group of **7**. Scale bar is 1 nm. The motion picture is shown in Movie S9, and enlarged images in Figure S9. Reprinted with permission from Ref. [19]. Copyright 2008 American Chemical Society.

der Waals interactions. It is possible that the last structure includes a second molecule of **7**, but the present level of space and time resolutions did not allow us to determine what exact changes took place.

The conformer after the large motion features a 1.0 nm stem (arrow, Figure 11) connecting the CNH and a new cyclic structure. Comparison with the molecular structure of **7** suggests that this stem is the aminocaproic acid residue of the molecule and that the dark "knot" next to the stem is the carbonyl group of the amide bond in the middle of the molecule.

The still and movie images shown in Figure 9–11 imply a new possibility for structural analysis, because SMRT-TEM imaging allows us to study the structural mobility of the conformers located in various local minima individually and simultaneously (Scheme 2). The structural information given by the SMRT-TEM is the location of the nuclei of individual molecules (conformers) with little vibrational perturbation. This quality of information is different from that given by the conventional methods of analysis of molecular ensembles or single molecules. For instance, the NMR data are for either an ensemble, equilibrium average in solution, or for the molecule frozen in local minima in solid. Single-crystal diffraction data give us the molecular structure of the average of a frozen ensemble in a crystal. Scanning probe microscopy provides an electronic image of single molecules fixed on a flat surface and as viewed only from the top.

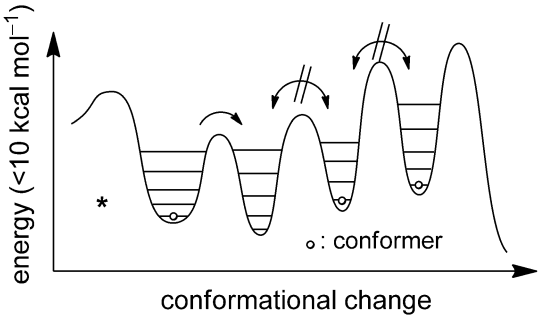

Scheme 2. Potential surface for conformational change.

6. A Mixture of Mobile van der Waals Molecular Clusters

An unusual aspect of the SMRT-TEM technique is that it can be applied to a mixture of substances of different molecular composition. This advantage is best illustrated for the structure determination of van der Waals clusters that have no structural periodicity and can be obtained only as a mixture of clusters with different molecular compositions. The challenge would be major particularly if the clusters were structurally mobile. We came across this challenge during our studies on the mechanism of heterogeneous nucleation of organic crystals.[14] In the study, we used the dibromophenylbenzamide molecule on a CNH (**5**) as a molecular template

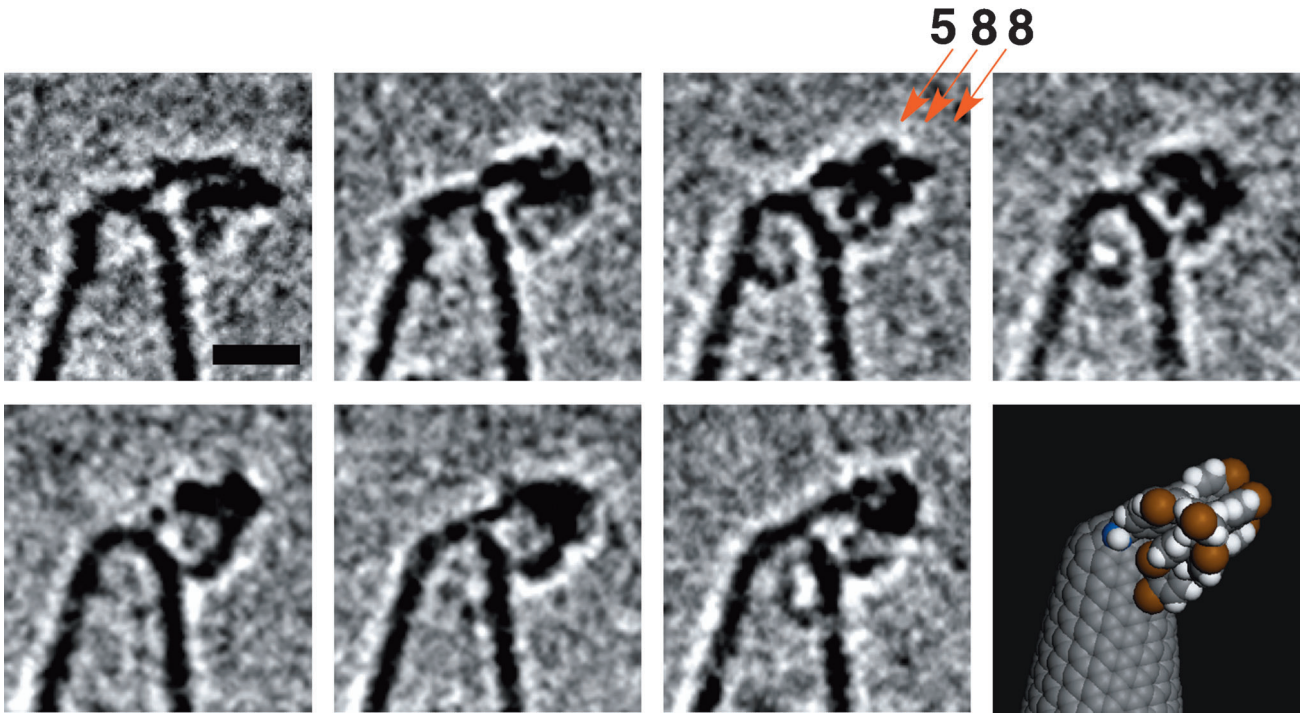

Figure 12. Termolecular [**5**+**8**$_2$] cluster on a CNH composed on one Y′ template and two Y molecules, observed with a time interval of 8.4 s (E = 120 kV), and a molecular model of a plausible structure of clusters. The total electron dose during the observation was 9.0×10^5 electron nm^{-2}. The cluster formed during recrystallization of **8** over **5**, and was recovered by filtration for TEM analysis. Scale bar is 1 nm. The motion picture is shown in Movie S10, and enlarged images in Figure S10. Adapted from Ref. [14].

for crystallization of the C_3-symmetric molecule **8** in ethanol. After crystallization in ethanol, we recovered the template from the crystallization solution, analyzed it using TEM and found many van der Waals clusters composed of two to a dozen molecules **8** sticking to **5** (denoted [**5**+**8**$_n$]).

Figure 12 shows several frames from a movie of such a molecular cluster ([**5**+**8**$_2$]). Careful analysis of each frame of the movie combined with theoretical modeling allowed us to conclude that two molecules of **8** are trapped between the benzamide moiety and the CNH surface of **5** by van der Waals interactions.

Figure 13 shows a larger cluster composed of **5** and **8**, totaling about 15 molecules ([**5**+**8**$_{14}$]). About 10 molecules form a mobile disordered core and several cover the core as a unimolecular-thick film. It appears that the core part gains periodicity during the imaging. The SMRT-TEM thus provided a rare opportunity to consider and visualize the fate of an individual small molecule in a fluid, and demonstrate the ability of atomic resolution SMRT-TEM imaging to provide such an unusual insight into the mechanism of nucleation and crystallization.

7. Molecular Translation in a CNT

7.1. Translation of Alkyl Carborane in a CNT

In retrospect, we were extremely lucky to have been able to record the first movie of the dialkyl carborane **1** in Figure 1, because it was one of the only two moving molecules that we could clearly identify. The vast majority of the molecules were either translating rapidly back and forth in the tube, or packed densely in the CNT and hence hardly analyzable. Figure 14a illustrates an example of a didodecyl carborane **2** moving quickly first to the top and then to the bottom (note that the top/bottom notation is only for the sake of Figure presentation and has not physical meaning). Because of the rapid translation during the irradiation period of 0.5 s, the molecular images are blurred. In Figure 14b, we plot the positions of the head and the end of the tail at 2 s intervals.

It is rather amusing to see how the molecule **2** moved in the tube. At time 0 s, it was in the center, at time 10.5 s it was moving rapidly (blurred image in the top of the tube), and at time 10.5 s, the head reached position 12.5 nm. At time 21 s, the head was at position 6.1 nm and the tail at position 2.0 nm; the apparent molecular length is as long as 4 nm because of rapid motion during the 0.5 s irradiation period. Between time 17 s and 46 s, the tail did not go beyond position 2 nm where there was a defect (red triangle). At time 48 s, the molecule went over the defect and stood still until the end of the observation. The motion was entirely stochastic and provided intriguing information on the "roughness" of the interior of the CNT. From this analysis, we expect that our instrument can detect molecule **2** if it translates at a speed slower than 5 nm s^{-1}.

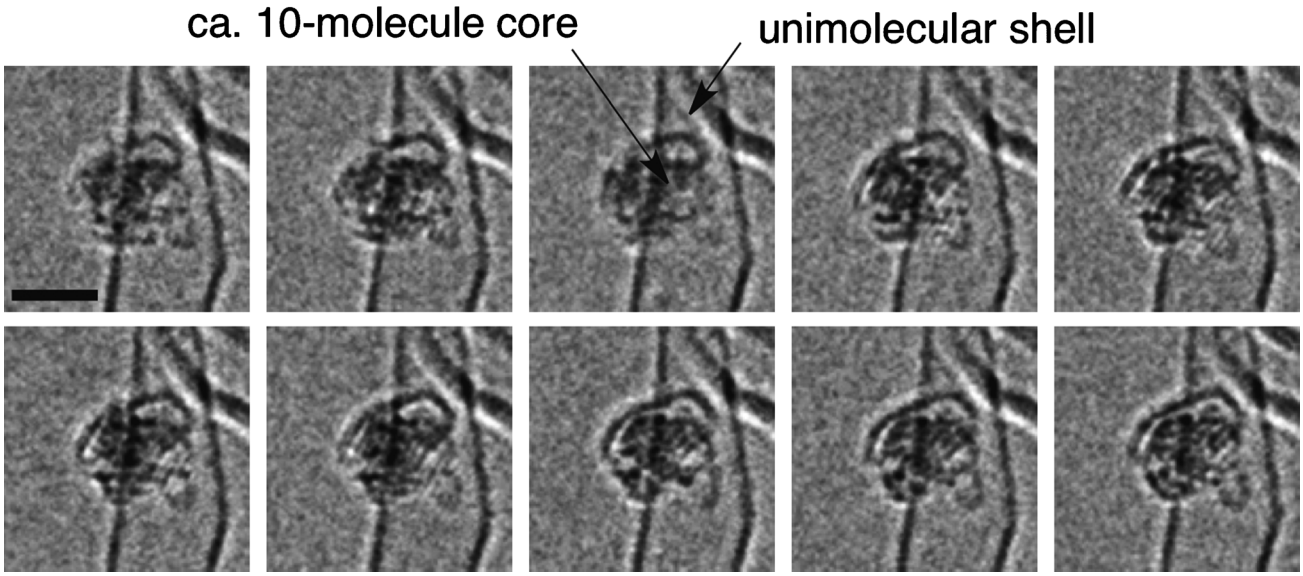

Figure 13. [5+8$_{14}$] cluster composed of about 15 molecules, which are observed with a time interval of 2.1 s (E = 120 kV). The total electron dose during the observation was 3.6×10^5 electron nm^{-2}. Scale bar is 2 nm. The motion picture is shown in Movie S11, and enlarge images in Figure S11. Adapted from Ref. [14].

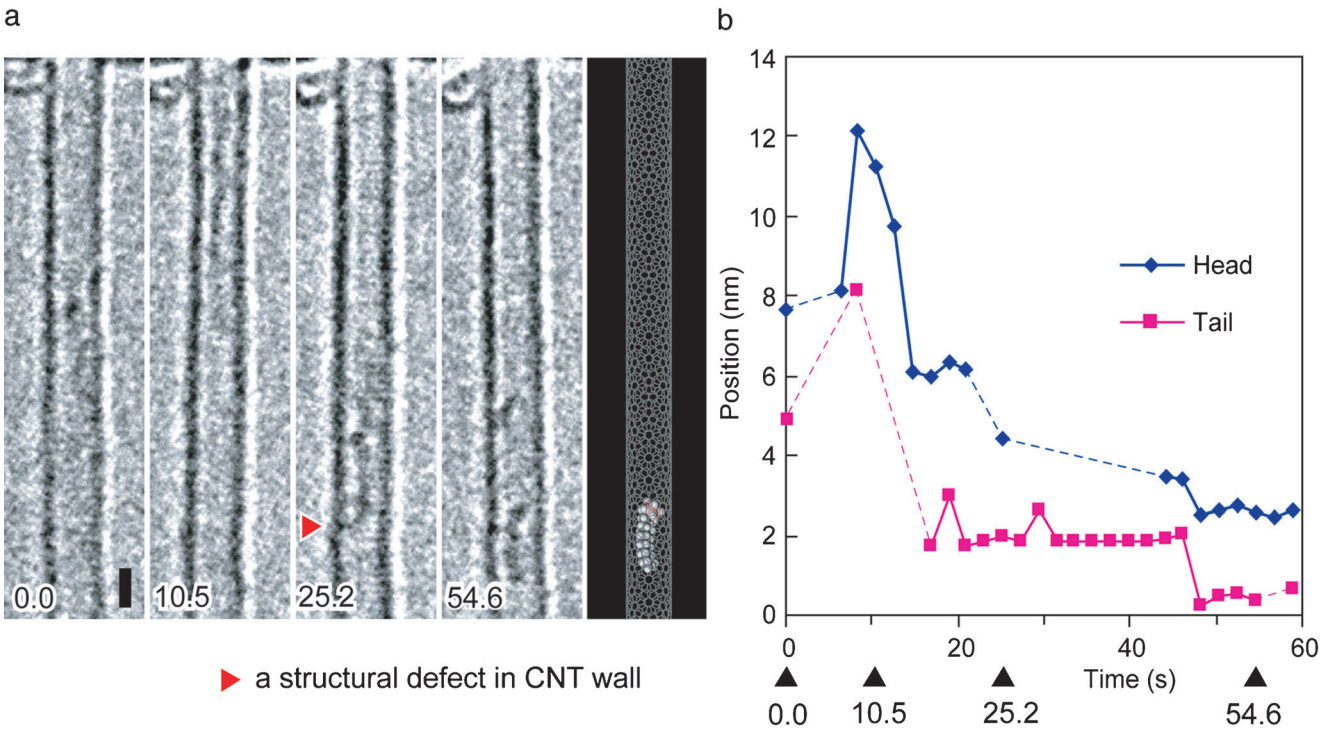

Figure 14. Translation of didodecyl carborane **2** through a CNT of 1.2 nm diameter without changing the orientation of the molecule (E = 120 kV; electron dose = 4.0×10^4 electron nm^{-2} frame^{-1}). The total electron dose from the beginning of electron irradiation (0 s) until time 54.6 s was 1.0×10^6 electron nm^{-2}. The scale bar is 1 nm. a) TEM images at the times indicated and a molecular model at 54.6 s. b) Numerical analysis of the translation of **2** through a CNT of 1.2 nm diameter. Time-dependent locations of the molecule. *x* axis: time in seconds after the start of imaging (0.5 s imaging and 1.6 s readout time intervals). *y* axis: position in nm. The black triangles mark the time of the images in (a). The motion picture is shown in Movie S12, and enlarged images in Figure S12. Adapted from Ref. [4].

7.2. Collision at 793 K Preceding One-Dimensional Bimolecular Reaction

Collision is the first essential step in bimolecular reactions. Do molecules react as soon as they collide with each other? or do they collide many times before they actually start to react with each other? This sounds like an unusual question indeed. How can we study such a question experimentally? [60]Fullerene molecules (**9**) in a CNT provide a rare showcase where we can study the one-dimensional collision (this Section) and

a subsequent intermolecular reaction (Section 8.1).[21] Fullerene molecules in a CNT may collide with each other with various molecular orientations (note the presence of pentagons and hexagons in fullerenes) to form a van der Waals complex, which then form one, two, and multiple bonds (Scheme 3). The processes between the first collision and the two bond formations were found to occur reversibly, and, beyond the two-bond stage, the irreversible multibond formation (i.e., fusion) took place in a dimer to form a fully-fledged C_{120} dimer.

Figure 15 illustrates a number of [60]fullerene (**9**) molecules in parallel CNTs placed on a 793 K stage.[21] The molecules in the tube in the top look as if they move at their own free will. We see stochastic molecular motions and collisions under a one-dimensional environment[11] and also an ensuing dimerization reaction. The molecules shown with a red arrow in Figure 15 (a peanut-shaped dimer) are partly fused. The trimer, apparently composed of a monomer and a peanut dimer (green arrow), moved together throughout the movie. In the beginning of the movie, the monomer shown with a blue arrow in Figure 15 may be trapped by a defect in the tube wall. In the third row, the peanut dimer (red arrow) and trimer rapidly (blurred image) approached the monomer from the left. In the bottom row of Figure 15, an apparent hexamer formed for several seconds, and then the monomeric fullerene bounced to the extreme right while the dimer and the trimer moved together to the left. This temporary intermolecular contact may be a van der Waals interaction or reversible bond formation. This movie, taken at 793 K, shows the very small temperature effect on the molecular translation that is qualitatively faster than those observed at 4 K (Section 3.2) and 293 K (Section 7.1), but still far slower than what is expected on the basis of the Arrhenius equation.

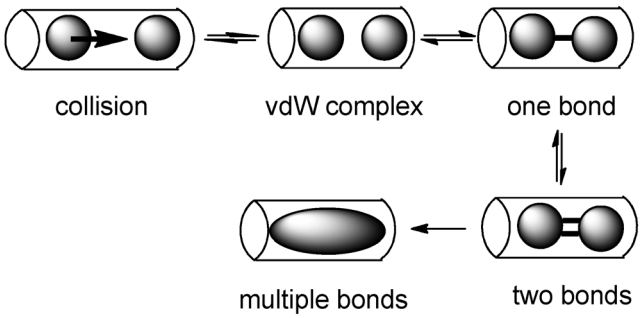

Scheme 3. Reversible collision, bonding, and irreversible fusion of two molecules.

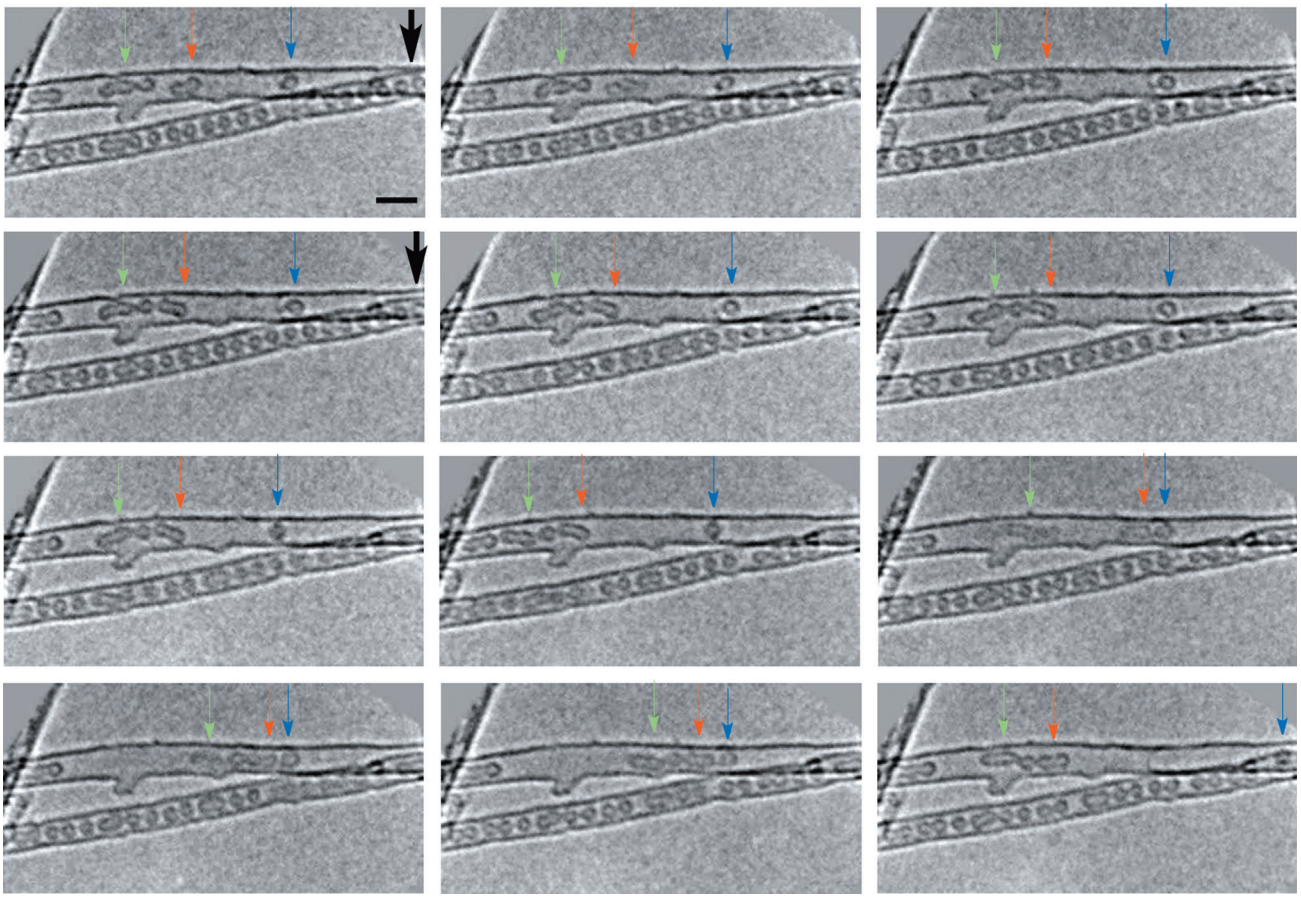

Figure 15. [60]Fullerene molecules (**9**) bonding in a CNT on a sample stage at 793 K with total electron dose over 1×10^6 electron nm^{-2} in the end ($E=120$ kV). The time interval between frames is 6.3 s. No apparent decomposition of the molecules and CNTs was observed in spite of the high temperature and substantial total electron dose. Scale bar is 2 nm. See text for details. The motion picture is shown in Movie S13, and enlarged images in Figure S13. Adapted from Ref. [21].

As seen from the images of the area indicated by black arrows in Figure 15 and in other areas as well, the CNTs vibrated by several Å. This vibration, however, was quite slow, as indicated by the lack of blurring during the 0.5 s exposure time (see by contrast the blurred fullerenes in the third row of Figure 15).

8. Imaging Uni- and Bimolecular Chemical Reactions at Atomic Precision

8.1. Stereoselectivity of Bimolecular Reaction Probed at Atomic Precision

In Section 7.2, Figure 15, we have seen a monomer, a peanut-shaped dimer, and a trimer bouncing against each other. The trimer, composed of a monomer and a dimer unit, maintained its structural integrity throughout the 1 min observation time. On the other hand, the monomer–dimer–trimer complex seen in the bottom of Figure 15 dissociated into two parts after several seconds. How does "interaction" evolve into "bonding"? The SMRT-TEM images provide a rare opportunity for us to ponder this important question.

Examination of many pairs of fullerene molecules indicates that some pairs dimerize quickly while some do not, suggesting a stereospecificity for dimerization. Indeed, there are two possibilities for dimerizing [60]fullerene (**9**) (Scheme 4). Connection of a double bond between two

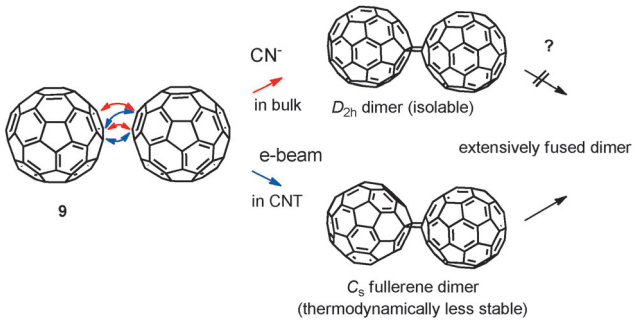

Scheme 4. Two pathways of [60]fullerene dimerization.

hexagons in each molecule (red arrows in Scheme 4) generates a D_{2h} dimer. This is the product of fullerene dimerization reactions under basic conditions in the solid, and reverts back to [60]fullerene upon single-electron oxidation or treatment with slow electrons (e.g., mass spectrometry).[22] The second pathway (blue in Scheme 4) generates a C_s dimer, which is thermodynamically less stable by about 20 kcal mol^{-1} (PM3 and B3LYP/6-31G*), and it is this isomer that was found to go further to the formation of the peanut dimer illustrated in the movie in Figure 16.

Figure 16 illustrates the dimerization of [60]fullerene molecules after they have met each other several times. The first picture is the C_s dimer that is illustrated in the bottom panel of Figure 16 as a molecular model. The reaction is reversible up to this stage, and beyond this intermediate, more extensive and irreversible bond reorganization took place, eventually forming the peanut dimer that is shown as a molecular model in the bottom right of Figure 16.

8.2. A New Reaction: Single-Metal Catalyzed C–C Bond Reorganization

With the SMRT-TEM technique, we could study the hypothetical reaction shown in Scheme 5 mediated by a single iron atom. In the reality shown in Figure 17,[23] a single bucky ferrocene molecule **10** rapidly underwent extensive bond

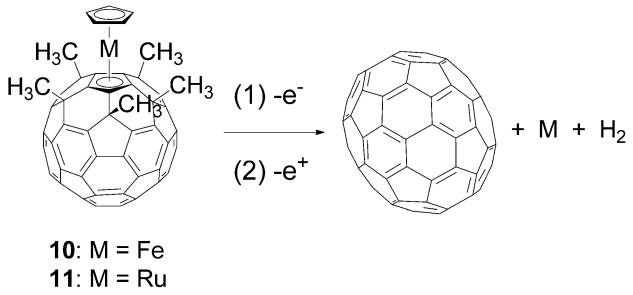

Scheme 5. A hypothetical reaction: $C_{60}(CH_3)_5(C_5H_5)Fe \rightarrow C_{70} + 10\,H_2 + Fe$.

reorganization to give a [70]fullerene-like molecule complexed with an iron atom. This is a new reaction discovered under the TEM conditions. Parallel observation of 23 bucky ferrocene molecules indicated that, in addition to [70]fullerene formation, the molecules underwent two additional reactions with nearly equal possibilities: that is, iron-catalyzed dimerization similar to the uncatalyzed dimerization we discussed in Section 8.1, and fusion with the CNT wall similar to those catalyzed by multimetallic clusters. Thus, TEM imaging allowed us visually to study the selectivity of the catalytic reaction. In the corresponding bulk experiments where the molecules have numerous neighbors, the fullerene molecules underwent polymerization in addition to C–C bond cleavage and formation reactions that gave isolable ferrocene derivatives.[24]

The clearly visible molecular image of molecule **10** on the right (blue arrow, Figure 17) in the first frame has already eroded in the next frame. The most notable change at this point is the disappearance of [60]fullerene's spherical image and the growth of an ellipsoidal structure (orange arrow, Figure 17) reminiscent of half of a [70]fullerene on the side closer to the iron atom. The new structure was stable once formed. The tight peapod packing that prevents migration of molecules and atoms among the cavities of the peapod compartments guarantees us that this structure has grown intramolecularly out of the [60]fullerene cage and the CH_3 and cyclopentadienyl groups, catalyzed by the iron atom originally a part of **10**. Therefore, we consider that the product is a molecule structurally similar to [70]fullerene.

The catalytic effects of the metal atom were apparent from comparison with the dimerization of [60]fullerene

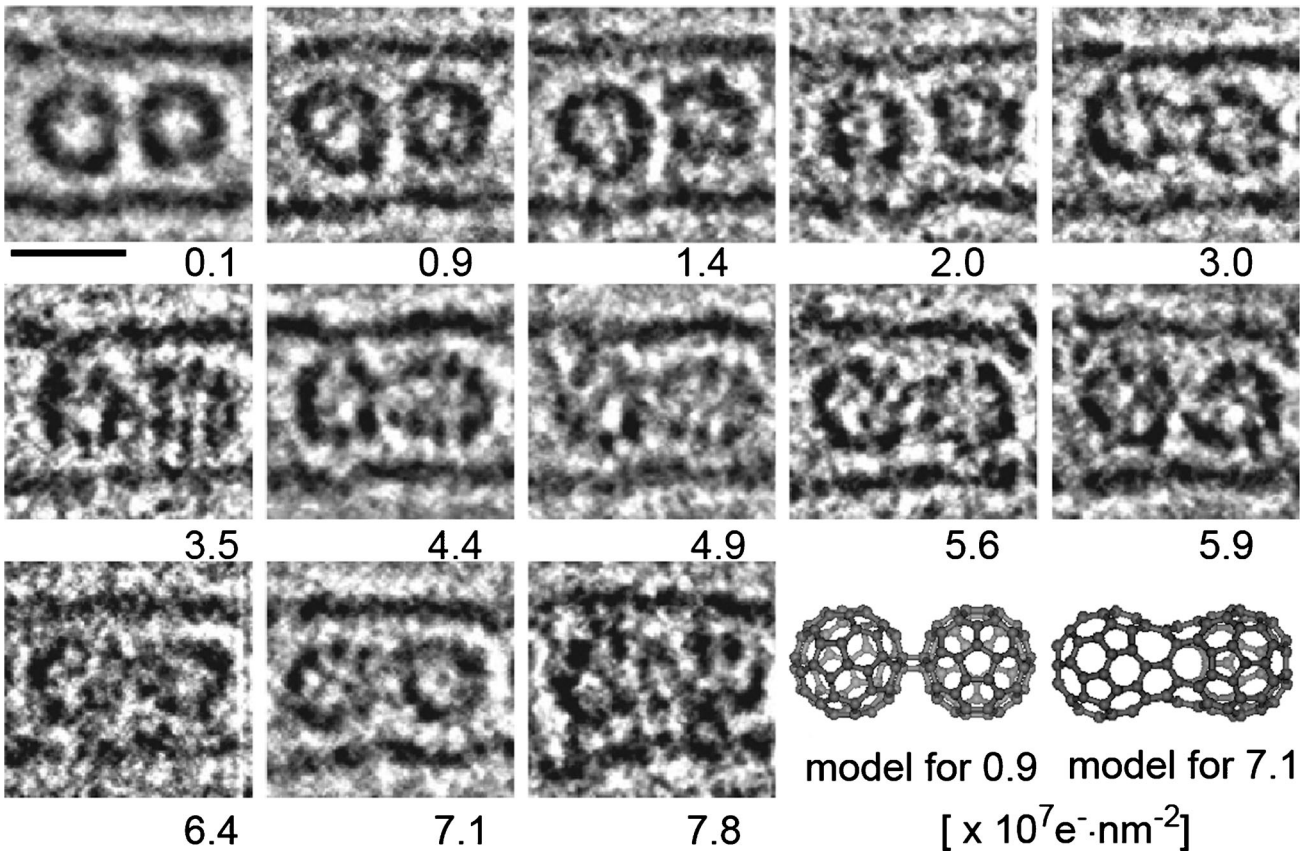

Figure 16. Course of dimerization of [60]fullerene (**9**) occurring during 4 min under the standard TEM conditions, as observed with a time interval between each frame of 9 s to 30 s ($E = 120$ kV). The total electron dose is shown below each frame. The motion picture is shown in Movie S14, and the enlarged image is in Figure S14. Adapted from Ref. [21].

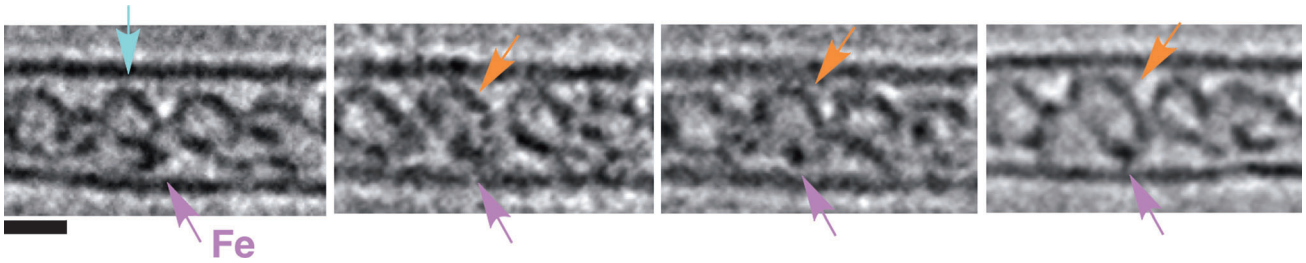

Figure 17. Conversion of bucky ferrocene **10** to a [70]fullerene-like molecule ($E = 120$ kV). The frames are shown to 21.0 s with a time interval between each frame of 4.2 s, the image in the fourth frame was taken with a total electron dose of 1.6×10^6 electron nm^{-2} after irradiation with 3.7×10^4 electron nm^{-2} for each frame taken. The motion picture is shown in Movie S15, and enlarged images in Figure S15. Reprinted with permission from Ref. [23]. Copyright 2011 American Chemical Society.

discussed in Section 8.1, which required a total electron dose as high as 3.0×10^7 electron nm^{-2}. In contrast, the reactions of bucky ferrocene **10** and bucky ruthenocene **11** required about 1000 times lower electron dose. The ferrocene started to show signs of decomposition after the first frame with 3.7×10^4 electron nm^{-2}, and the bucky ruthenocene (**11**) had decomposed already at this dose. Such high catalytic activity of these metals in C–C bond reorganization has been noted in the study of Fischer–Tropsch and steam-reforming reactions.[25] This discovery may also give some clues to the study of the elusive mechanism of iron-catalyzed synthetic reactions.[26]

8.3. Ionization Potential and Chemical Reactivity

The SMRT-TEM images of organic molecules discussed in the foregoing Sections illustrated our capacity for studying the static and dynamic structural changes of single organic molecules. The images of stable organic molecules could be obtained for a few minutes until a total dose of $> 1 \times 10^6$ electron nm^{-2}, above which the CNT container may start to decompose. These stable molecules have a large ionization potential (IP) (i.e., a low HOMO level) and hence are resistant to electron irradiation: for example, benzene (ca. 9 eV), olefin (10 eV), amide (10 eV), hydrocarbon (13 eV),

and perfluorocarbon (18 eV). In contrast, molecules with a low IP value (i.e., a high HOMO level) decompose much faster than the high-IP molecules. They include a tertiary amine (8 eV),[27] fullerenes (6.5 eV),[21] CNT (4.9 eV), and ferrocene (4.74 eV),[28] which have been found to undergo structural change under TEM conditions. CNTs that hold the molecules have a very low IP and with a large total cross section of collision are highly susceptible to ionization even upon impact with fast electrons (note that the faster the electron, the smaller the cross section of the collision, as has been known since J. J. Thomson's time). Therefore, we expect that the electron beam preferentially ionizes the CNT, and the ionized CNT serves as a catalyst for the reactions of the nearby molecules following the well-known mechanism of cation radical catalysis.[29] A few other examples in addition to those discussed above are noteworthy in this context: the reaction of a tertiary amine with the wall of the CNT generating an EELS spectrum suggestive of the formation of a quaternary ammonium salt,[27] the alleged *cis*/*trans* isomerization of trisubstituted olefin,[30] and bond reorganization of CNT by multimetallic clusters.[31]

9. Summary and Outlook

A series of frames of atomic resolution movies of the motions and reactions of organic molecules and molecular clusters illustrate the unusual potential of SMRT-TEM imaging in molecular science. For light atoms, such as carbon, hydrogen, and oxygen atoms, the TEM conditions are mild enough to allow us to observe van der Waals clusters of aromatic compounds such as **8**, and to study the conformational changes of a rather complex molecule such as biotin triamide **7**. For molecules that have a high IP value, such as hydrocarbons and amides, we can study their structure and motions for several minutes. For those with a low IP value, such as fullerene and ferrocene, we can study the course of their reaction, which is probably catalyzed by the ionized CNT under the cation radical catalysis mechanism.

Recording the molecular motions over time, the movies provide richer structural information than the still pictures. Like a movie in a theater, the two-dimensional movie can give us three-dimensional information as the molecule rotates spontaneously on or in the CNT, and this four-dimensional information can be obtained for many molecules together with the EELS data on their elemental composition. Thus, the quality of the "4D + 2" information gained by SMRT-TEM imaging differs significantly not only from that obtained by analysis of molecular ensembles such as diffraction and spectroscopy, but also from single-molecule analyses such as scanning probe microscopy and high-resolution optical microscopy. The movies of a mixture of molecules and clusters have proven to serve as an unusually powerful method for the study of the molecules on a solid surface, for example, that of the mechanism of crystal nucleation.[14] With the advance of TEM technology, especially with improved time and space resolution, SMRT-TEM imaging will become a powerful sub-nm-scale analytical method that can be carried out on a single molecule.

The development of the SMRT-TEM technique depended crucially on a few boundary conditions that have received little previous attention. To observe the molecules in vacuum, we fixed them in the viewing field of the TEM by bonding them to a CNT, and we found that the molecular motions occur on the time scale of seconds and the speed of the motions is essentially insensitive to the temperature of the sample stage—the key factor for our discovery. Qualitatively speaking, the behavior of the molecules on a CNT is between that of the molecules fixed tightly on a substrate for scanning probe microscopy, and those in vacuum for spectroscopic studies where the molecules vibrate in the order of picoseconds. The chemical bonding of the specimen molecule on the outside CNT is a method of choice for higher image resolution because it fixes the molecule in vacuum, and for the reliability of the chemical fixation of the molecule to the CNT. Encapsulation in a CNT is simpler but limited in scope, because the molecules need to be small and to have high affinity to the interior of the CNT. CNTs and CNHs have so far been the substrates of choice for their robustness as a single-atomic film and for the conductivity that prevents sample charging. Graphene sheets may also serve for the purpose.

The SMRT-TEM imaging of small organic molecules in vacuum has challenged the accepted wisdom of the TEM community that organic molecules decompose quickly under irradiation with as small an electron dose as 10^3 electron nm^{-2}.[6,32] Our discovery suggests that this accepted wisdom applies only when the TEM specimen is a solid that has a very large cross section of collision, and has a small IP, such as CNT, fullerene, ferrocene. For a solid sample, the energy of the electron beam is effectively transferred to the solid to cause ionization of the molecules and disruption of molecular ordering. The resulting molecular ions in the solid undergo quick reactions with the nearby molecules. In contrast, a single organic molecule in vacuum has a very small cross section of ionization, and is known to be hard to ionize efficiently by fast electrons.[33] The ionized molecules in vacuum cannot undergo intermolecular reactions except receiving electrons from the high-lying HOMO of the CNT and returning to the neutral state.

It was in the middle of the 17th century that Robert Hooke illustrated in his *Micrographia* small objects such as a flea and "cells" in cork (Figure 18).[34] With this book, he pointed out the new world of the Science of Nature, which in his opinion was a work of the Brain and the Fancy. Before the invention of the microscope, the flea was just a black moving object of unknown nature, and the discovery of "cells" paved the way to modern biology. Is SMRT-TEM imaging going to play important roles in molecular science? Perhaps it will do so. One possible field would be the analysis of a mixture of molecules, for which there has been little hope of obtaining precise structural information. Crystal nucleation discussed in Section 6 is the first example of this kind. Mobile protein structure is another challenging target that may immediately occur to the minds of readers.[6] With the ever-increasing spatial resolution thanks for the development of monochromatic light sources and aberration correctors as well as forthcoming improvement of time resolution, we expect that

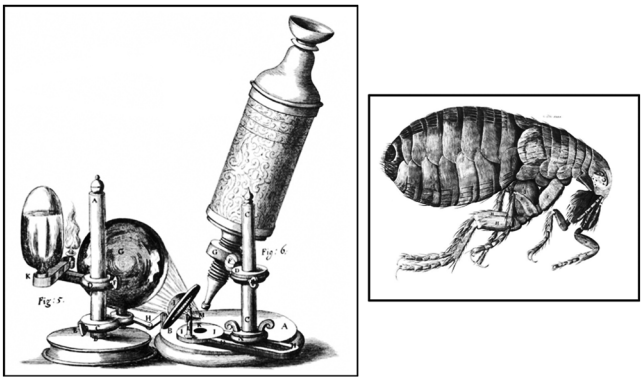

Figure 18. Robert Hooke's optical microscope and flea from *Micrographia* (1665) (http://www.gutenberg.org/files/15491/15491-h/15491-h.htm).

much of the resolution problems would be resolved in the near future. In addition, it is not unlikely that the rapidly developing environmental TEM technique allows us to study in situ the reaction of gaseous molecules with a single molecule fixed on a solid surface. The SMRT-TEM movies will also prove to be an effective tool for chemical education in high school and junior high school. Chemistry has indeed already been too long made only of a work of the Brain and the Fancy, and hence it is too abstract for school children to like it. One junior high school textbook of chemistry in Japan published in April 2012 shows a frame of the movie in Figure 1. Is SMRT-TEM going to produce more chemistry enthusiasts among young generations?

We appreciate the experimental and intellectual contributions of the able co-workers whose names are found in the text and the references, in particular the ERATO TEM members, Drs. K. Suenaga, M. Koshino, and Y. Niimi, for their expertise in TEM. We also thank Prof. K. Yamanochi for insightful discussions and Dr. K. Harano for help in the preparation of the molecular pictures. Insightful comments on the history of conformational analysis by Prof. J.-M. Lehn is deeply appreciated. We thank MEXT for financial support (KAKENHI, No. 22000008), and the Japan Agency for Science and Technology for the ERATO Project (2004-2010) where the continuous support from JEOL Ltd. was instrumental in the successful execution of the project.

Received: July 17, 2012

[1] H. Sachse, *Ber. Dtsch. Chem. Ges.* **1890**, *23*, 1363 – 1370.
[2] E. Nakamura in *Gakumon no Tobira* (*A Door to Learning*) (Eds.: J. Hamada, T. Kadowaki, M. Gonokami, A. Matsui, T. Yoshimi), Kodansha, Tokyo, **2007**, pp. 332 – 343.
[3] E. Nakamura in *Chemistry of Nanocarbons* (Eds.: T. Akasaka, F. Wudl, S. Nagase), Wiley-VCH, Weinheim, **2010**, pp. 405 – 412.
[4] M. Koshino, T. Tanaka, N. Solin, K. Suenaga, H. Isobe, E. Nakamura, *Science* **2007**, *316*, 853 – 853.
[5] T. Kobayashi, S. Isoda, *J. Mater. Chem.* **1993**, *3*, 1 – 14.
[6] W. H. Massover, *Micron* **2011**, *42*, 141 – 151.
[7] A. Hashimoto, H. Yorimitsu, K. Ajima, K. Suenaga, H. Isobe, J. Miyawaki, M. Yudasaka, S. Iijima, E. Nakamura, *Proc. Natl. Acad. Sci. USA* **2004**, *101*, 8527 – 8530.
[8] M. Koshino, N. Solin, T. Tanaka, H. Isobe, E. Nakamura, *Nat. Nanotechnol.* **2008**, *3*, 595 – 597.
[9] B. W. Smith, M. Monthioux, D. E. Luzzi, *Nature* **1998**, *396*, 323 – 324.
[10] Z. Liu, K. Yanagi, K. Suenaga, H. Kataura, S. Iijima, *Nat. Nanotechnol.* **2007**, *2*, 422 – 425.
[11] J. H. Warner, Y. Ito, M. Zaka, L. Ge, T. Akachi, H. Okimoto, K. Porfyrakis, A. A. R. Watt, H. Shinohara, G. A. D. Briggs, *Nano Lett.* **2008**, *8*, 2328 – 2335.
[12] T. W. Chamberlain, A. Camenisch, N. R. Champness, G. A. D. Briggs, S. C. Benjamin, A. Ardavan, A. N. Khlobystov, *J. Am. Chem. Soc.* **2007**, *129*, 8609 – 8614.
[13] O. O. Adisa, B. J. Cox, J. M. Hill, *Nanoscale* **2012**, *4*, 3295 – 3307.
[14] K. Harano, T. Homma, Y. Niimi, M. Koshino, K. Suenaga, L. Leibler, E. Nakamura, *Nat. Mater.* **2012**, *11*, 877 – 881.
[15] H. Isobe, T. Tanaka, R. Maeda, E. Noiri, N. Solin, M. Yudasaka, S. Iijima, E. Nakamura, *Angew. Chem.* **2006**, *118*, 6828 – 6832; *Angew. Chem. Int. Ed.* **2006**, *45*, 6676 – 6680.
[16] A. H. Zewail, *Science* **2010**, *328*, 187 – 193.
[17] N. Solin, M. Koshino, T. Tanaka, S. Takenaga, H. Kataura, H. Isobe, E. Nakamura, *Chem. Lett.* **2007**, *36*, 1208 – 1209.
[18] T. Okazaki, Y. Iizumi, S. Okubo, H. Kataura, Z. Liu, K. Suenaga, Y. Tahara, M. Yudasaka, S. Okada, S. Iijima, *Angew. Chem.* **2011**, *123*, 4955 – 4959; *Angew. Chem. Int. Ed.* **2011**, *50*, 4853 – 4857.
[19] E. Nakamura, M. Koshino, T. Tanaka, Y. Niimi, K. Harano, Y. Nakamura, H. Isobe, *J. Am. Chem. Soc.* **2008**, *130*, 7808 – 7809.
[20] D. Tasis, N. Tagmatarchis, A. Bianco, M. Prato, *Chem. Rev.* **2006**, *106*, 1105 – 1136.
[21] M. Koshino, Y. Niimi, E. Nakamura, H. Kataura, T. Okazaki, K. Suenaga, S. Iijima, *Nat. Chem.* **2010**, *2*, 117 – 124.
[22] G. W. Wang, K. Komatsu, Y. Murata, M. Shiro, *Nature* **1997**, *387*, 583 – 586.
[23] E. Nakamura, M. Koshino, T. Saito, Y. Niimi, K. Suenaga, Y. Matsuo, *J. Am. Chem. Soc.* **2011**, *133*, 14151 – 14153.
[24] T. Nakae, Y. Matsuo, M. Takagi, Y. Sato, K. Suenaga, E. Nakamura, *Chem. Asian J.* **2009**, *4*, 457 – 465.
[25] J. R. Rostrup-Nielsen, J. Sehested, J. K. Nørskov, *Adv. Catal.* **2002**, *47*, 65 – 139.
[26] E. Nakamura, N. Yoshikai, *J. Org. Chem.* **2010**, *75*, 6061 – 6067.
[27] Z. Liu, M. Koshino, K. Suenaga, A. Mrzel, H. Kataura, S. Iijima, *Phys. Rev. Lett.* **2006**, *96*, 088304.
[28] L. Guan, Z. Shi, M. Li, Z. Gu, *Carbon* **2005**, *43*, 2780 – 2785.
[29] N. L. Bauld, D. J. Bellville, B. Harirchian, K. T. Lorenz, R. A. Pabon Jr. , D. W. Reynolds, D. D. Wirth, H. S. Chiou, B. K. Marsh, *Acc. Chem. Res.* **1987**, *20*, 371 – 378.
[30] Ref. [10].
[31] T. W. Chamberlain, J. C. Meyer, J. Biskupek, J. Leschner, A. Santana, N. A. Besley, E. Bichoutskaia, U. Kaiser, A. N. Khlobystov, *Nat. Chem.* **2011**, *3*, 732 – 737.
[32] Ref. [5].
[33] L. S. Bartell, E. A. Roth, C. D. Hollowell, K. Kuchitsu, J. E. Young, *J. Chem. Phys.* **1965**, *42*, 2683 – 2686.
[34] http://www.gutenberg.org/ebooks/15491.

